M. Preisinger

Resonant Excitation of Magnetostrictive Driven Print Wires for High-Speed Printing

Abstract: A developmental resonant wire printing device utilizing ultrasonic vibration is described and results given on some preliminary work on the resonant excitation of magnetostrictive print wires. This paper discusses the characteristics of the magnetostrictive material, the transducer design and some special methods of measuring small, rapid mechanical motion. In the present test setup of the printing device, impact rates up to 1400/sec were obtained.

Introduction

The application of piezoelectric materials to high-speed printing or recording and the use of resonant excitation was first described by French inventors[1] in 1936, who also mentioned the possibility of replacing these piezoeletric materials by magnetostrictive media. At that time, however, little had been published on transducer design and the generation of high-power ultrasonics. Later, Mason,[2] Van der Burgt,[3] Neppiras,[4] and Eisner and Saeger[5] established the fundamental design rules, primarily considering the steady-state operation of mechanisms driven at ultrasonic frequencies. When using such a device for high-speed printing (i.e., >1000 impacts/sec), however, the transducer does not have constant input impedance and the print element is never at constant amplitude. The wholly transitory character of the desired rapid motion requires special characteristics for the transducer material, the transducer design and the measuring devices required for this type of development work. These characteristics will be discussed in this paper and some recent results in the development of a high-speed printing technique will be shown.

The recording media used in conventional high-speed printers are the type wheel, drum, chain, stick and wire mechanisms. At present the upper limit for wire matrix printing is about 200 char/sec. The other types of high-speed printers, which are limited by the positioning time for type bars or slugs, operate up to about 50 char/sec.

In the development work to be reported here the ultrasonic vibration method was studied because it appears to offer several attractive advantages over conventional printing techniques. These advantages are included among the following features, which were apparent from the outset:

1. It would involve a minimum of moving parts and a minimum of maintenance.
2. The desired print amplitudes could be developed in a in a short time, offering the potentiality of high operating speeds.
3. Multiple copies could be made in a single run.
4. Ordinary paper could be used.
5. Application in both parallel and serial printers would be possible.
6. The noise level would be lower than that of solid-type impact printing.

The character of ultrasonic vibrations does not permit the attachment of wheel, chain, or stick mechanisms, and so the use of "engraved type" printing (type slugs or bars) is not possible. The potential speed can be utilized only in matrix printers.

This paper will discuss the rationale for the choice of the ultrasonic technique and the results of some preliminary work on resonant excitation of magnetostrictive print wires.

Printing principles

The basic form of the *conventional wire printer* is a group of wires, each in a guiding tube, usually arranged in a 5×7 matrix. One end of the wires is close to a platen on which rests a paper and a carbon ribbon. The opposite end of the wires can be actuated by cams, hammers or clutches that propel the wire in parallel motion towards the paper.

A *magnetostrictive printer* would consist of a magnetostrictive wire rigidly fastened to one end of a nonmagnetic guiding tube and surrounded by a drive coil. Dc current

through the coil would cause a magnetostrictive action, driving the tip of the wire against the carbon paper resting on the platen. In practice, however, the print wire would have to be very long (several meters) for known magnetostrictive materials, and the thermal coefficient of expansion would introduce severe operating problems.

The *resonant wire printer* consists of a relatively short wire driven at its longitudinal resonant frequency by a drive coil, as indicated in Fig. 1a. The length of the wire would have to be such that for a single peak amplitude of about 0.2 mm in a printing process, the stress intensity of the wire would be below its endurance limit. The wire fastened at the end opposite the print station to a relatively large mass would be excited in the quarter-wavelength mode.

Figure 1 Principle of the resonant wire printer. (a) General configuration. (b) Longitudinal resonant excitation of a magnetostrictive rod.

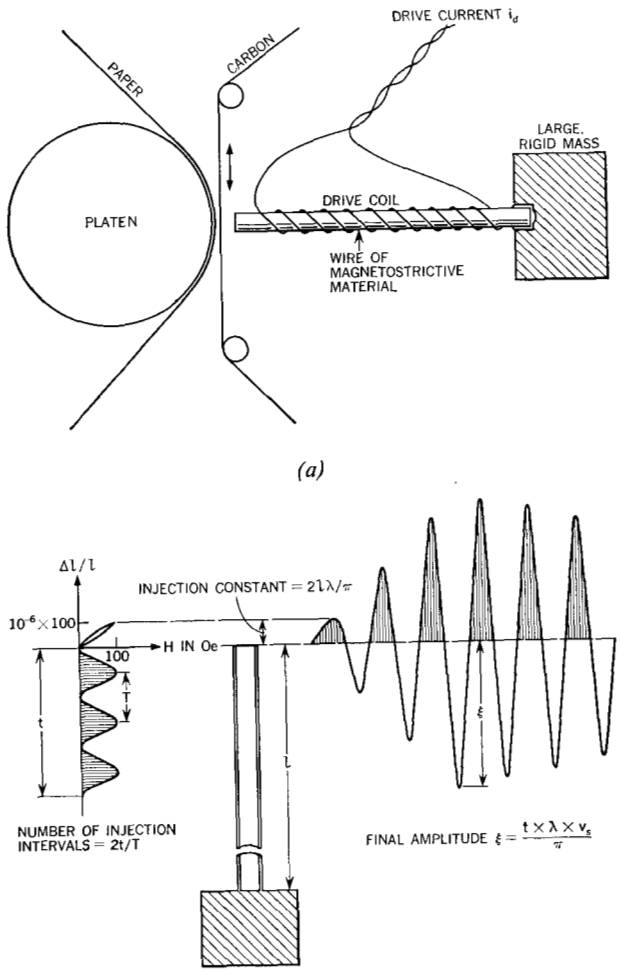

The mechanical Q, which is the ratio of energy stored in the resonator to energy consumed by the resonator per cycle, should be in the order of 1000 and higher; therefore, few losses exist and the wire temperature remains constant at various printing speeds. One solution would be to use a wire of magnetostrictive material e.g., an Co-Fe alloy. Such materials, however, are difficult to draw into wire and have to be annealed before use, resulting in brittleness (in the particular case of Co-Fe) and low fatigue strength; they develop magnetic hysteresis losses that would overheat the wire at high printing speeds; and they also take too long to develop the desired amplitude for a high-speed print device.

Figure 1b serves to show the function of such a device when driven for a time $t < \tau$ (where τ = time constant of the resonator). With T as the duration of a period and t the drive time required for one impact, a total of $n = 2t/T$ injections is obtained, representing the first of two important expressions for the final amplitude ξ. The second factor, which could be termed "injection constant K," is given by

$$K = l \cdot \lambda \cdot 2/\pi$$

in which

l = length of wire

$\lambda = \Delta l/l$ = static coefficient of magnetostriction

$2/\pi$ = a constant, accounting for the sinusoidal distribution of the motion along the wire.

The final single peak amplitude ξ is then given by:

$$\xi = n \cdot K = 2\,\frac{t}{T} \cdot l \cdot \frac{\Delta l}{l} \cdot \frac{2}{\pi}. \tag{1}$$

Inserting into Eq. (1) the expression

$$f = \frac{1}{4l}\sqrt{\frac{E}{\rho}},$$

in which

f = resonant frequency of a quarter wavelength piece

E = modulus of elasticity

ρ = density of the material

with $\sqrt{E/\rho}$ being the velocity of sound v_s in the magnetostrictive material we finally obtain

$$\xi = \frac{t \cdot \lambda \cdot v_s}{\pi}. \tag{2}$$

This shows that for a given injection time the developed amplitude depends only on the static coefficient of magnetostriction and the velocity of sound in the magnetostrictive material.

Applying this knowledge to the previously discussed direct magnetostrictive-driven resonant wire printer, the amplitude ξ obtained with practical values of 350 μsec

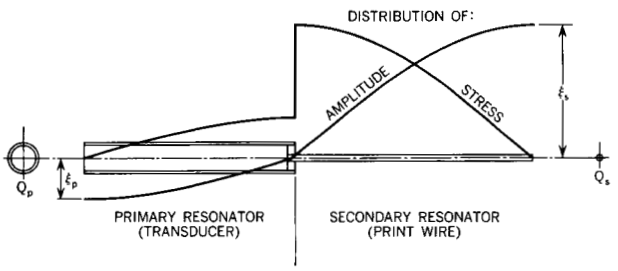

Figure 2 Schematic print element and its important parameters. The transducer, 49 Co, 49 Fe, 2 V (cut under 45° to rolling direction) features high static magnetostriction at low magnetization, high coefficient of electromechanical coupling, and high energy storage. The print wire (Ti alloy) features low energy storage and is a high-strength, wear resistant material.

for drive duration, 45×10^{-6} for λ and 5×10^{6} mm/sec for v_s is 0.025 mm, which would be inadequate for a practical device. The directly magnetostrictive driven element, which has been discussed by Buser[6] and Preisinger[7] would not seem to have practical possibilities for high-speed printing.

The *indirectly driven resonant print wire* is an alternate approach using a wire of nonmagnetostrictive material coupled to some sort of electromechanical transducer, preferably a magnetostrictive type. This solution allows the use of a high-strength material for the print wire and highly magnetostrictive materials for the transducer shown in Fig. 2. However, it doubles the associated resonating mass, and therefore the drive energy, since the compound resonator must at least be equal to a half-wavelength. We will see later on that this disadvantage can be avoided but we will first examine the fundamental compound resonator. Provided the secondary resonator (the print wire) of Fig. 2 is coupled properly to the primary resonator (the transducer), an amplitude transformation is obtained according to the relation

$$\xi_s = \xi_p \sqrt{Q_p/Q_s}, \tag{3}$$

where

ξ_s = single peak amplitude of secondary resonator
ξ_p = single peak amplitude of primary resonator
Q_s = cross-section of secondary resonator
Q_p = cross-section of primary resonator

In practice, a cross-section ratio of 100 : 1 does not pose any difficulties, and provides an effective single-peak amplitude of 0.25 mm. The design properties of the two main parts of this print element will now be studied.

Magnetostriction and magnetostrictive materials

The foregoing review indicates the basis for developing a single-wire print element for high-speed operation. Such a device would obviously require a high static coefficient of magnetostriction, high electromechanical coupling factor and low losses. Before discussing the design considerations we will briefly review the fundamental processes occurring when a magnetic material is in a magnetic field. Magnetization takes place in two characteristic intervals[8] according to the kind of domain distribution more or less sharply defined in the material. The region of spontaneous domain-switching accounting for the 180° turns of domains is followed by rotational processes in which the domains are turned in the direction of the magnetic field.

Kneller[9] has given a clear explanation of effects associated with magnetostriction, according to which a 180° turn does not change the length of a single crystal or a domain and consequently very little or no magnetostriction is observed within this interval, as can be seen from Fig. 3, which shows a magnetostriction curve above the magnetization curve. Both curves were taken at the same time from the same specimen of soft, annealed nickel. From this behavior one can anticipate that any operation on the material which would cause an orientation of the single domains is associated with a change of the magnetostrictive properties. To evaluate this, the magnitude of the magnetostriction was measured on hard-rolled Co-Fe sheet with the probes cut at different angles β to the direction of rolling, as shown in Fig. 4a. The reduction in area due to cold working was in the order of 90%. The samples were rolled to tubing and annealed for two hours at 800°C.

As a result of cold working, a preferred orientation of the magnetostriction appears at 45° to the angle of rolling. Figure 4b shows the results obtained from two samples of the same material having a different degree of cold work. The magnetostriction was measured at a magnetization of 60 Oe. For sample B, for instance, the 45° cut has 40% higher magnetostriction than the 90° cut probe, whereas for sample A the increase is 50%. Figure 5a demonstrates this drastic effect on a sample of Co-Fe, which was cut under 45° to the direction of rolling with practically no magnetostriction present in the range of domain switching

Figure 3 The fundamental relation between induction and magnetostriction. Specimen: hard drawn nickel.

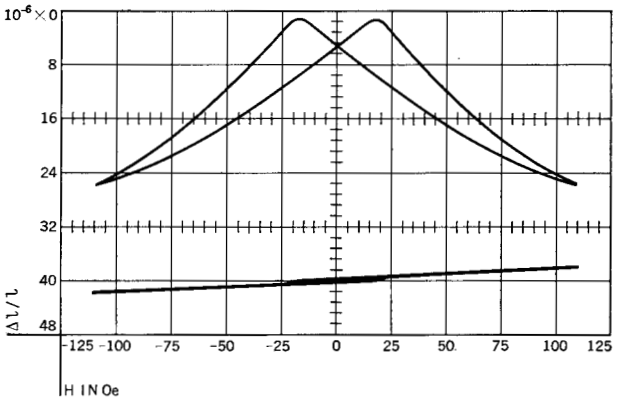

but with a high and linear change in length when the rotation processes start. Figure 5b shows the behavior of the same probe in the interesting magnetization range of ~100 Oe. A fixed amount of dc premagnetization in Fig. 6a and a single minor loop is shown in Fig. 6b. All measurements were made at 50 cps. The fact that higher magnetostriction exists in hard drawn, 45° cut material also results in a drastic increase of the electromechanical coupling factor K^2, known to be the ratio of mechanical energy $\frac{1}{2}E(\Delta l)^2$ obtained from the transducer to electrical energy $B \cdot H/8\pi$ applied to the transducer

$$K^2 = \frac{\frac{1}{2}E(\Delta l)^2}{B \cdot H/8\pi}. \tag{4}$$

With high degrees of cold working, Δl increases to 150% and the modulus of elasticity decreases to 65% but the resulting coupling factor K^2 still shows a considerable increase at 45° cutting angle. In practice, a K^2 of 0.25 was realized, which is high for magnetostrictive type transducers. These experiments were the first step to obtain a high-performance, single-wire print element.

Figure 4 (a) Selection of probes to determine the influence of the cutting angle β. (b) Static magnetostriction in 49 Co, 49 Fe, 2 V versus the cutting angle.

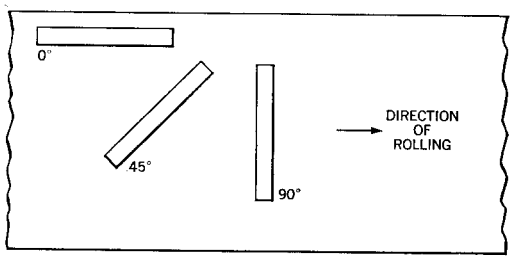

(a)

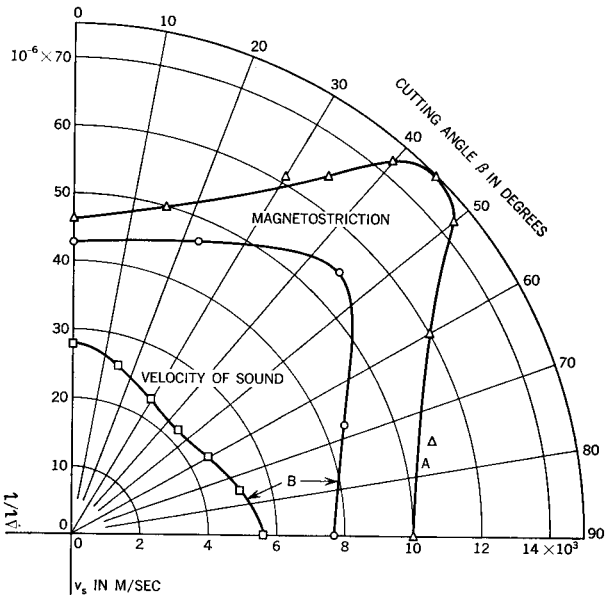

(b)

Longitudinally resonating print wire

At this point we had achieved a good electromechanical coupling factor but had not demonstrated sufficient amplitude, since according to Eq. (2) the single print amplitude ξ is, even with the 45° cut material, still only 0.04 mm. In dynamic applications the increase in λ due to the 45° cut cannot be fully used since at the same time the velocity of sound was reduced from 5000 to 4000 m/sec. As explained earlier we have to make use of amplitude transformation to obtain the desired value of $\xi = 0.2$ mm. This amplitude is limited only by the fatigue limit of the material used for the print wire. In the case of carbon spring steel wire, an alternating stress value of 50 kg/mm^2 should not be exceeded. With the natural frequency of 12×10^3 cps the length l of the wire becomes $l=(1/4f)\times v_s=105$ mm. For a modulus of elasticity of 20,000 kg/mm^2 and a sinusoidal stress distribution, the actual created stress in the wire is

$$\sigma = E\frac{\Delta l}{l}\frac{\pi}{2}$$

$$= 20{,}000 \times 1.9 \times 10^{-3} \times \pi/2 = 60 \text{ kg/mm}^2.$$

With completely undamaged material this stress intensity would be possible, but in practice little irregularities and scratches could cause ruptures. It is therefore desirable to reduce the stress in the resonator without affecting the amplitude/energy ratio in the negative direction. The steady-state user of an ultrasonic vibration does not care for this ratio; he has ample time to build up a certain amplitude and, once it is established, the electrical driver only has to deliver the energy consumed by the specific application the device is used for. He may even look for a transducer with particularly high storage to obtain little damping. When using a longitudinal vibration for printing, the energy stored in the resonator is much higher than the energy consumed by the actual print process; and since we have a pulsed application, it must be removed from the resonator right after a dot has been printed. Consequently, we must look for a resonator which has for a given amplitude as little energy storage as possible. This could also be achieved by the use of suitable titanium alloys, but no one up to this time has been able to produce titanium in wire shape with an almost polished surface—so in the specific case of our print wire, one cannot make use of the advantageous properties of titanium.

Consequently, spring steel wire has to be used, of which manufacturability is well under control. However, the particle velocity resulting from our amplitude and frequency still does not permit using the cylindrical shape.

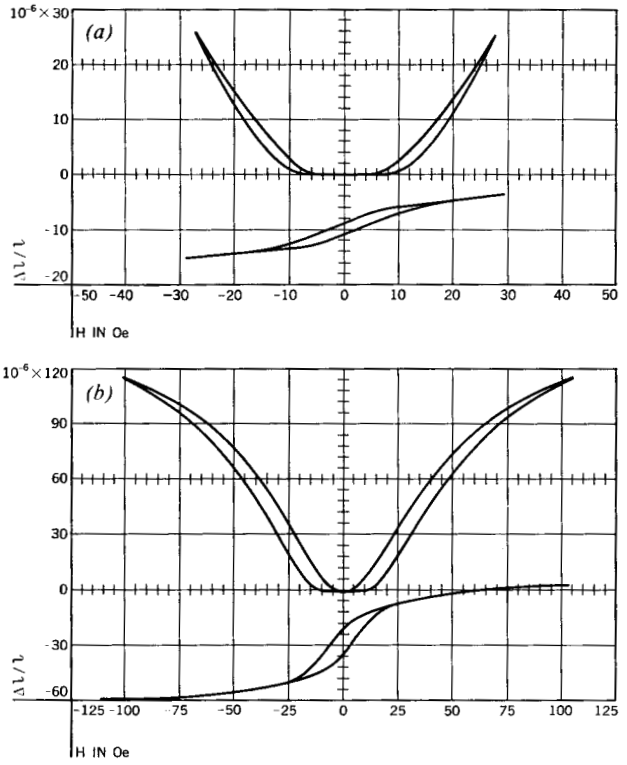

Figure 5 (a) Magnetostriction and induction in 49 Co, 49 Fe, 2 V. (b) Magnetostriction in same alloy. The induction loop is shown for reference.

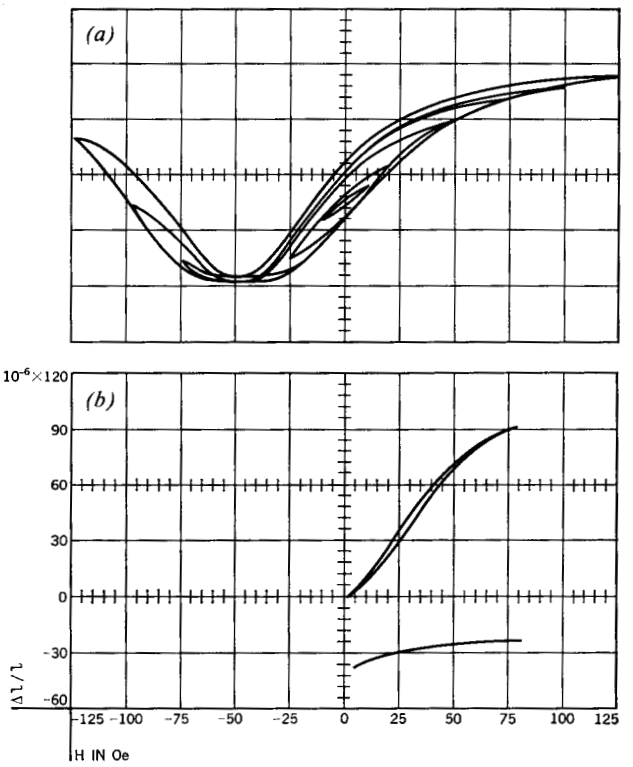

Figure 6 (a) Magnetostriction loops with fixed dc bias and several degrees of alternating flux density. (b) Minor magnetostriction loop of Co-Fe.

There are many ways of tapering known to reduce stress[4] but only that degree of taper that creates unit stress in every single particle of the entire resonator can be expected to give, with unit energy, a maximum of amplification. This device is known as a "constant stress" or "Gaussian" type resonator.

In case of mechanical forming, as milling or drawing, the constant-stress shape can be approximated only in steps, allowing a certain modulation depth of stress along the resonator, as shown in Fig. 7. A disadvantage of this stepwise transformation is that if the shape were obtained by drawing, different strength exists in each stage as an effect of different working factors. Also, the edges cause wear in the guiding tube that has to be used to prevent excessive parasitic transverse excitation. It is possible, however, and particularly useful, to use an electromechanical etching process for correct constant-stress shaping of the resonator. A byproduct of the electro-etching process is the highly polished surface, resulting in reduced wear of the guide material. The design chart, Fig. 8, contains all important data for any degree of tapering. Note that at a reduction in cross section to 59% the energy throughput in the resonator is highest.

Figure 7 Stress and amplitude distribution along a 9 stage, constant-stress resonator. Modulation depth 20%. Cross section reduction to 1/6. Dotted lines show distribution in an untapered resonator.

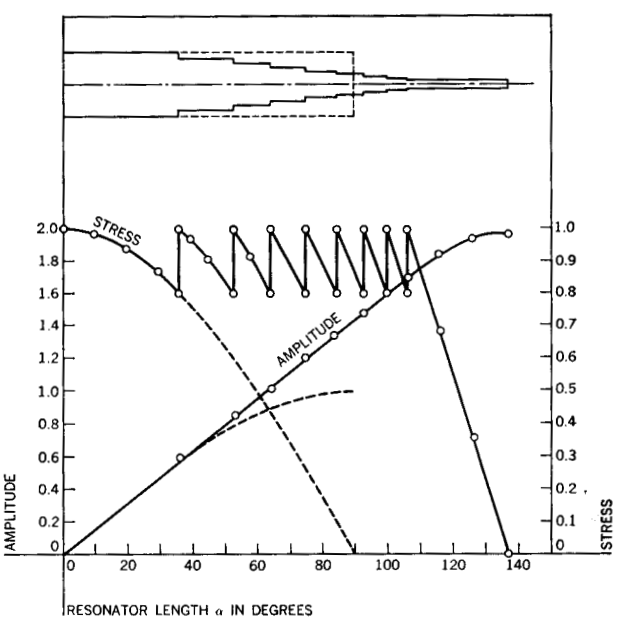

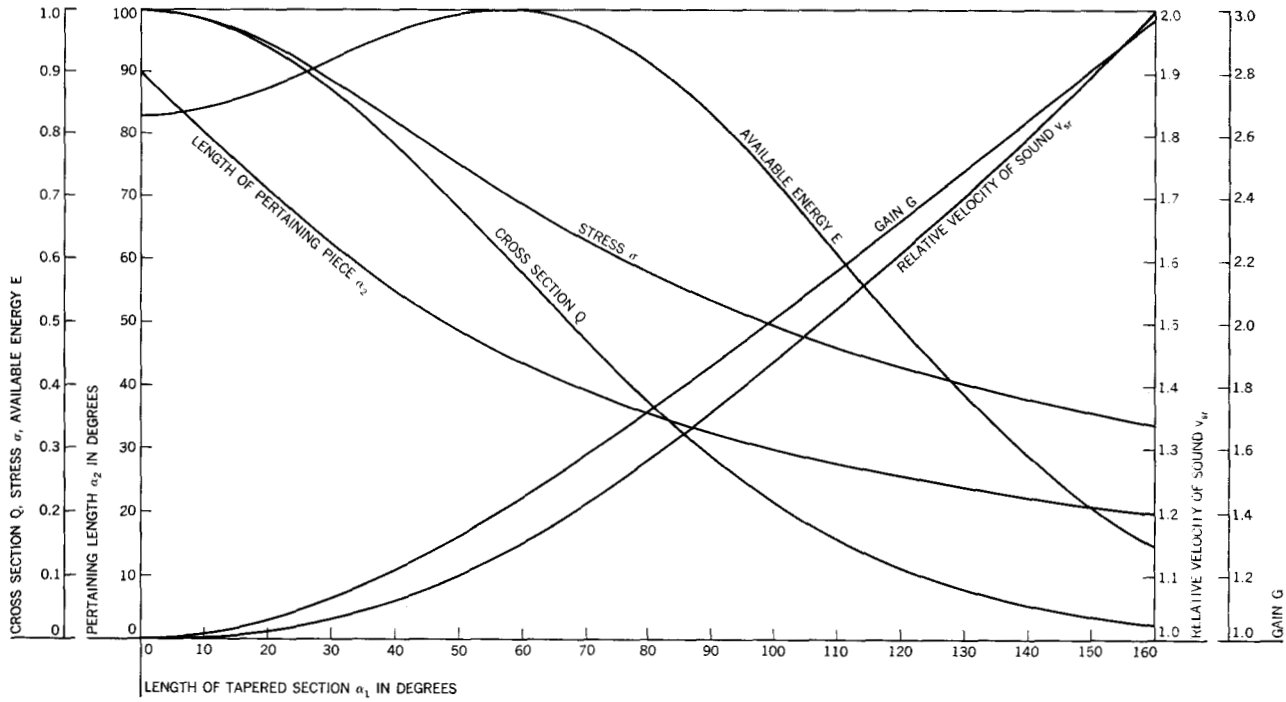

Figure 8 Constant stress resonator design chart. Start with the desired parameter, e.g., Gain = 2. Draw first a horizontal line from 2 until you hit the curve $G = f(\alpha_1)$, and second, a vertical line through this point over the entire diagram. The cutting point with the remaining curves will give the magnitude of the remaining parameters.

The guide for the tapered section is shaped as follows. Polyurethane is used as the guiding material. Best results have now been obtained when the clearance between the tapered print wire and the wall of the guiding channel is 0.025 mm. To insure that this clearance remains constant along the tapered print wire, an oversize print wire is etched and used as a mold when the guiding portion for a print head is cast. Removing the oversize wire after curing supplies the desired tapered guide tube.

Single wire element

The print wire is attached to the magnetostrictive transducer at a locus of impedance match. A mounting screw permits fastening the elements to print head assemblies. The fundamental element can be used in two variations or a combination of both to solve various printing problems which could be:

1. Single print head, having limited dimensions, operating at very high speed (1400-2000 impacts/sec) equipped with backward driven elements (Fig. 9a).
2. Combination of single print heads, operating at medium speed (~1000 impacts/sec) equipped with forward driven elements (Fig. 9b).
3. The pure parallel printer which requires highest packaging density and is obtained only by the alternate use of forward and backward driven elements (Fig. 9c).

Both the forward and backward driven elements are fundamentally the same. Their total cross-section change between primary resonator and the free end of the print wire is fixed to be 40:1. This change can be used either for

1. A pure cross-section transformation at the coupling point and no transformation in the cylindrical secondary resonator.
2. A zero cross-section transformation at the coupling point and a pure distributed transformation in the constant-stress tapered secondary resonator.
3. Any combination of (1) and (2).

There exists, however, a pronounced optimum for the final amplitude ξ as a function of the ratio of these two transformations, as can be seen in Fig. 10, which also shows the effective amplitude versus the ratio of transformation. The reason is obviously caused by the different nature of the two mathematical functions, which are responsible for the total gain, expressed by

$$G_T = \sqrt{\frac{Q_p}{Q_{s0}}} \cdot \sqrt{1 + 2 \ln \frac{Q_{s0}}{Q_{sE}}}, \tag{5}$$

where

Q_p = cross-section of the primary resonator
Q_{s0} = cross-section of the print wire at the fixed end
Q_{sE} = cross-section of the print wire at the free end.

The development effort to reduce stress in the secondary resonator has now brought it to the desired stress reduction

at the 70% stress point and has achieved an amplitude gain of 10%. The previously calculated stress value of 60 kg/mm^2 is here reduced to 42 kg/mm^2, which is very moderate for the material used for the print wire.

Some consideration has to be given to the drive coil that is used on the primary resonator—particularly in regard to length and distribution over the resonator. According to the energy-distribution along the resonator, following a $\sin^2$ function with its maximum at the node point, the highest coupling factor would be obtained with a short coil located at the node point. In practice, the length of the drive coil should be such that a high percentage of the maximum possible energy injection is accomplished according to the expression

$$E(\%) = 0.637\gamma + 0.3185 \sin 2\gamma \qquad (6)$$

with

E = Energy content of the resonator (under the assumption that with a 90° long drive coil 100% energy is coupled into the resonator)

γ = coil length in degrees (90° = quarter-wavelength).

Figure 11 shows that with 60° coil length, 94% of the energy has been developed in the resonator. The coil, therefore, need not be any longer than 60°.

It is also desirable, of course, to have a short element. This can be obtained when inefficient portions of the distributed primary resonator are replaced by a concentrated part (loading mass).

The use of a loading mass not only decreases the mechanical length of the resonator but also increases its energy content and it is desirable to have high energy storage in the primary resonator. Figure 12 allows one to determine the energy relations for any combination of distributed and concentrated elements. It shows also that the energy content of the resonator is highest when it is shortened to a resonator length α of 60°.

The half-wave resonator, at first glance, has a major disadvantage over the quarter-wave resonator: it needs twice the energy. In resonant-wire printing, the energy consumed by the printing process is negligible compared to the energy stored in the resonant wire. It is therefore desirable to have an element that stores as little energy as possible. In the conventional half-wave resonator, one cannot avoid having energy in both resonators but, by offset tuning of the two quarter-wavelength portions, a sweep can be created, causing the energy to pass forward and backward between primary and secondary resonator. Figure 13 shows the actual motion versus drive current in a resonator. It can be noticed that the primary resonator is completely energy-free when the secondary resonator has maximum amplitude. At this time, all the energy has been transferred from the injection portion to the print

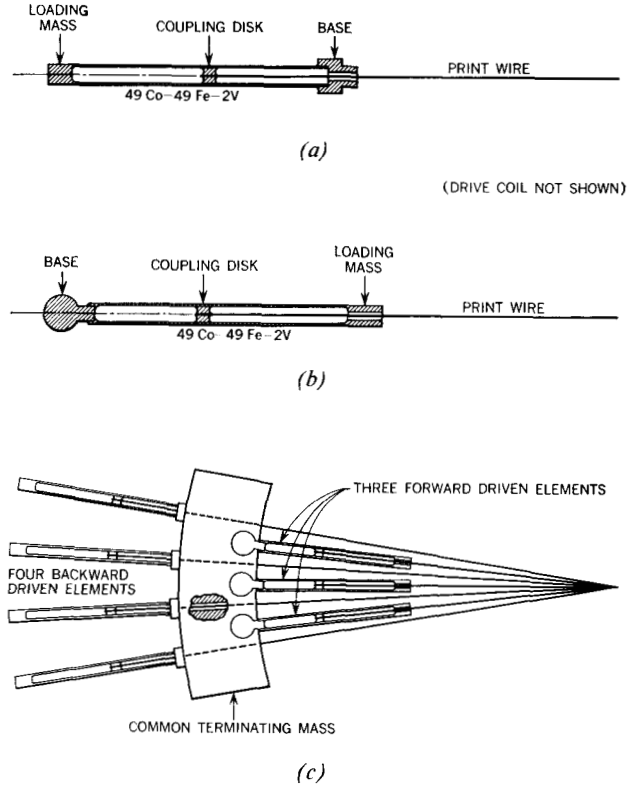

Figure 9 (a) The backward driven element.
(b) The forward driven element.
(c) Combination of forward and backward driven elements for highest packaging density.

Figure 10 Print amplitude versus transformation ratio.

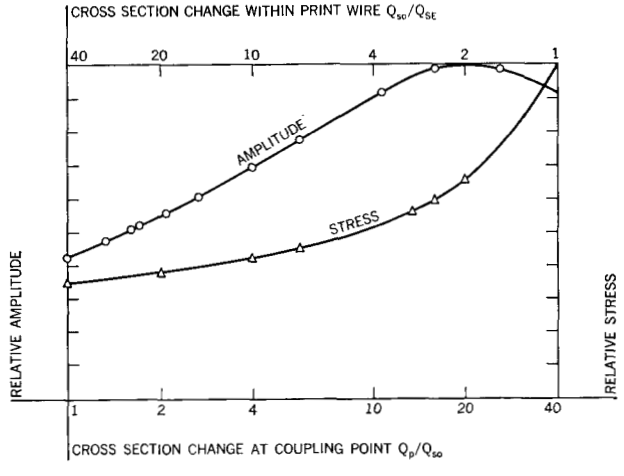

portion of the single-wire element. A typical motion of the print wire is shown in Fig. 14.

As can be seen from Fig. 14, the first maximum is followed by a number of reflections of which the first is the most undesirable, since it could cause the kind of multiple

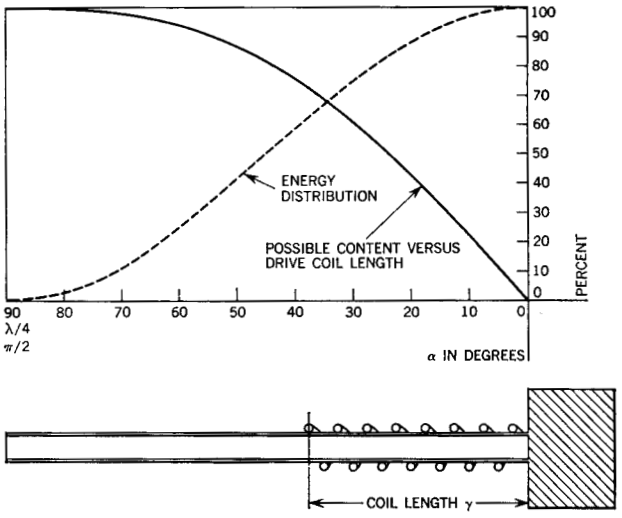

Figure 11 Energy distribution in resonator and energy-content versus drive coil length. α is resonator length.

Figure 12 The shortened longitudinal quarter wavelength resonator. In the abscissa α is the resonator length.

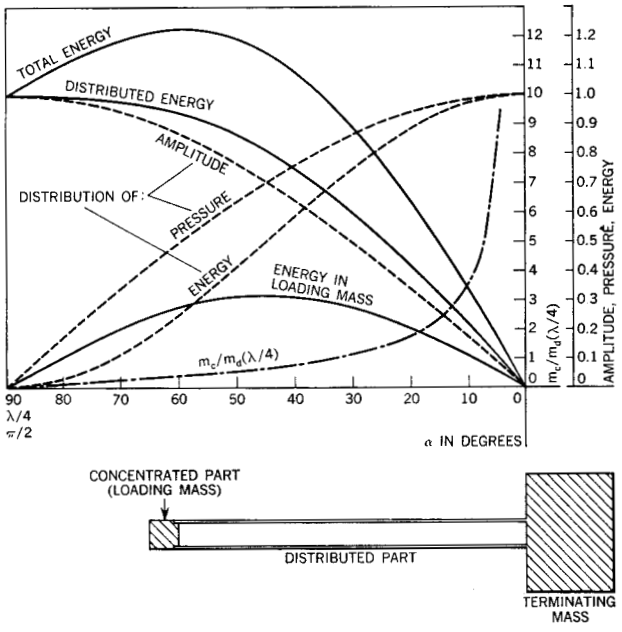

imprints known as "ghost printing." The condition first maximum/first reflection ≥ 4 should be satisfied.

With the natural damping of the element, this condition cannot be obtained, and so an additional damping is needed. Mechanical devices have the disadvantage of being unstable as a result of wear. The element, however, can be used as an electrical control of the decaying process by means of an antiphase brake pulse. This impulse is derived from the back-slope of the master drive pulse and delayed by such an amount of time that the newly injected energy is in antiphase with the stored energy of the element. By shifting the delay of the brake impulse in intervals of T, the point can be reached where both energies, the remaining stored energy of the element and the opposing injected brake energy, become equal and any further motion of the wire is cancelled.

• *Single wire drive*

For efficient operation of a single-wire drive, the large quantity of power applied to the element has to be generated as close to the print element as possible. A grounded-base oscillator was chosen for this purpose to

1. Avoid reversal of the feedback voltage.
2. Prevent changes in the frequency behavior of the transistor.
3. Key the device from low power logic circuitry.

The diagram is shown in Fig. 15.

This oscillator can be keyed with an input power of 20 mW and delivers an ac and dc magnetization to the resonator corresponding to 30 W over a duration of 350 μsec.

Print head assemblies

The print head is capable of very high speeds, but these speeds cannot be utilized in single position printing since special mechanisms would then be necessary to step the print head or the paper at speeds up to 1500/sec. But it can be used to obtain speeds of 200 char/sec with less cost and fewer parts, by incremental generation of the desired character. A developmental print head for 200 char/sec horizontal line printing has only four different parts. The paper stepping mechanism is omitted, since up to such speeds printing can be done on the fly.

With the print head assemblies currently developed, the horizontal character width can easily be changed by simply changing paper or print speed, respectively. By insertion of appropriate delays to different single-wire elements of a print head assembly, *tilted characters* can be obtained. The excellent possibilities of these print devices for plotting diagrams are evident. A number of possible print head assemblies are shown in Fig. 16 and print samples obtained with these heads at a character speed of 140/sec, corresponding to 1400 impacts/sec in Fig. 17. Carbon paper, preferably plastic carrier carbon, is used for inking. In the case of printing on multiple carbon sheets, a total of four copies has been obtained when the print head was in contact with the paper and the conventional ribbon was replaced by an additional carbon sheet.

Conclusion

Resonant wire printing allows high mechanical impact rates—1400/sec was employed successfully in present test equipment. The elements can be used in full matrix devices, being capable of printing 1400 char/sec, hard copy,

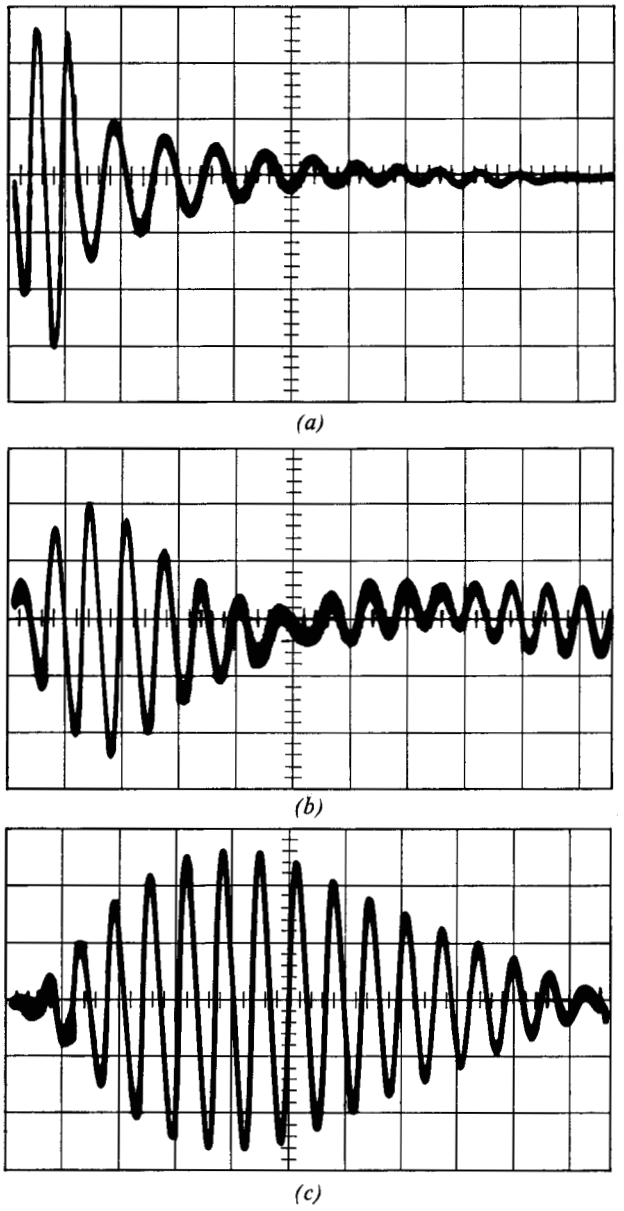

Figure 13 The offset tuned compound resonator. Note that the primary resonator is completely energy-free when the print wire has maximum amplitude. (a) Drive current vs time; (b) amplitude of primary resonator; (c) amplitude of secondary resonator.

with a single position. The problem of stepping either print head or paper at such speeds has not yet been solved. The potential advantages of this new printing technology have therefore been used for simplified print devices in the upper speed range of present wire printers. Such solutions are available in hardware, their characteristics being: low cost, speed of 200 char/sec, only seven mechanically moving parts, high reliability, and no requirement for paper stepping.

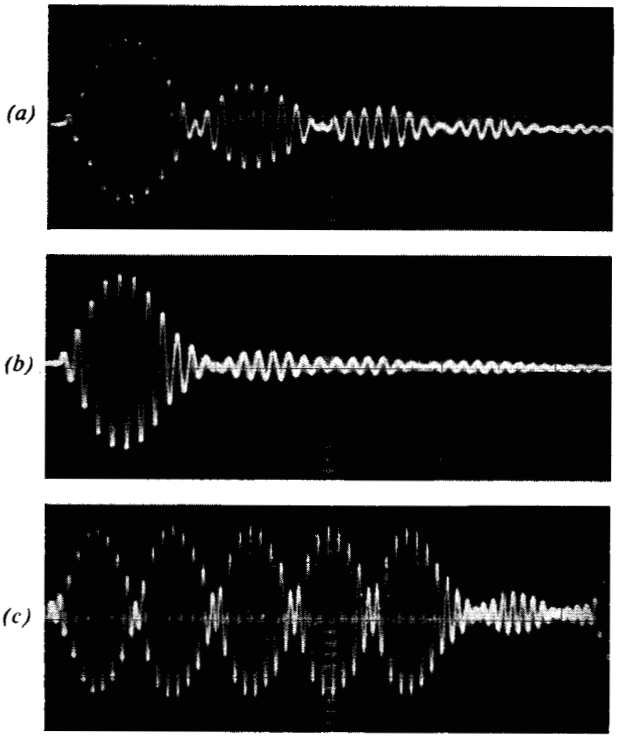

Figure 14 (a) Typical motion of a print wire. Decay natural, according to internal damping. (b) Same resonator as shown in (a) with antiphase brake impulse applied. (c) The same resonator pulsed for 1400 imp/sec; 5 out of 7 (to print a dash).

In the process of the development of this print device, unusual solutions had to be found in order to obtain a highly reliable and economical element. Key steps towards achieving this goal were:

1. The increase of the magnetostriction of the Co-Fe alloy (at 100 Oe magnetization) to 110×10^{-6}.
2. The increase of 36% in storage capacity of the primary resonator, when the resonator length is shortened to 60°.
3. The sweeping action of the compound resonator, which transports all the injected energy from the transducer portion to the print portion of the element.
4. The choice of the proper transformation ratio to obtain lowest energy storage in the constant-stress, tapered print wire.
5. The antiphase brake pulsing which, without any additional circuitry, permits the element to be re-driven every 714 μsec.
6. A unique measuring device for small and fast mechanical amplitudes [Appendix II], which is the key to success when dealing with minute changes of magnetostriction.

The application of these print devices requires ability to adjust to its particular characteristics, the most unusual of which is the limited stroke.

In the simplest case of single-copy printing on endless

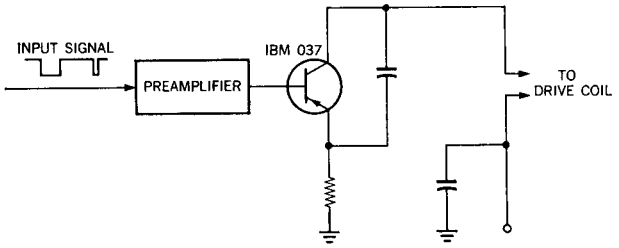

Figure 15 The drive circuit of a single wire element.

forms, no difficulties arise. When printing single copies on single sheets or cards, a rotating platen having a flat section for forms entry was found useful. In both cases the carbon can be run in any direction relative to paper flow. When printing on multiple carbon forms, however, the print head has to stay in contact with form and platen, in the same way as with electrochemical print devices.

The parameters achieved so far are not the ultimate obtainable. Improvements in speed and motion are possible by the use of low-energy-storing materials for the print wire, e.g., Ti-alloys and fiberglass rods. Also the reliability figure (0.5 CE h/20 $\times$ 10^6 char.) is only the initial result for a new technology.

Acknowledgments

The author wishes to acknowledge steadily received encouragement by Mr. W. Scheerer, valuable discussions with Mr. L. Reichl, the contributions of Mr. R. L. Zurowski, especially concerning the etching technique of the constant-stress print wire, and the work of his collaborators Messrs. Köberle, Kohler, Just, Tuerk and Rank.

Appendix I

This appendix deals with the design layout and results obtained with a VHF-transducer, particularly useful for the analysis of small mechanical motion. When converting a mechanical motion into a frequency modulation, followed by a high-Q ratio detector, an equivalent electrical voltage having low distortion can be obtained which may be observed with an oscilloscope. Sensitivities of 6 V/μm have been realized. The upper frequency limit of the mechanical motion is 100 kc/sec. Higher values can be reached at the expense of sensitivity.

The very special nature of a pulsed sonic or ultrasonic vibration calls for a special measuring device that does not load the specimen under test in any way, reacts fast enough to detect mechanical changes in the microsecond region and still delivers equivalent output voltages which can be traced on an oscilloscope.

The VHF-line oscillator was found to be useful for this purpose. If the device under test is brought in close proximity to the open end of the oscillator, the load capacitance resulting from the average distance A_s and the length of the coaxial line of characteristic impedance, Z_0, determine the frequency of the oscillator, which is inversely proportional to the line length L. Loading the line with a capacitance, C, however, simulates an additional piece of line length, proportional to

$$\Delta L = \frac{3}{100} \cdot C \cdot Z_0 \tag{A1}$$

leading to an effective line length

$$L_{\text{eff}} = L + \Delta L. \tag{A2}$$

One part of ΔL is due to the static loading of the line with the capacitance C_0 of the test device being at rest. When, however, the latter is energized to generate mechanical motion, a modulated portion according to

$$\Delta L_{\text{mod}} = \frac{3AZ_0}{400\pi} \left(\frac{1}{A_s - \xi} - \frac{1}{A_s + \xi} \right) \tag{A3}$$

is obtained. This leads to a frequency modulation of the oscillator, whose modulation depth is 44 kc/sec with values of 1 mm for A_s, 1 mm^2 for the effective area A, and 1 μm for ξ. The total change in capacitance, causing the 44 kc/sec frequency modulation is 1.6×10^{-5} pF.

The next task is to remove the frequency modulation from the carrier and to convert it into an amplitude modulation. The discriminator circuit is most suitable for this purpose. Two quarter-wavelength stubs are used, purposely laid out for maximum Q. They are both tuned to their point of inflection, one circuit above and the other below the center frequency of the oscillator. The associated

Figure 16 Several 7-element print heads, capable of printing 200 char/sec on the fly.

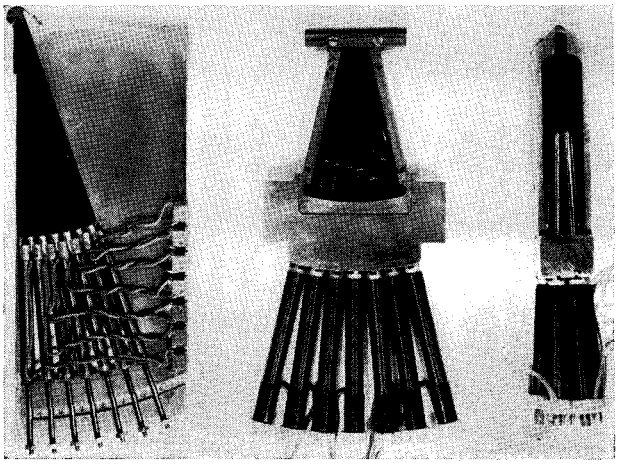

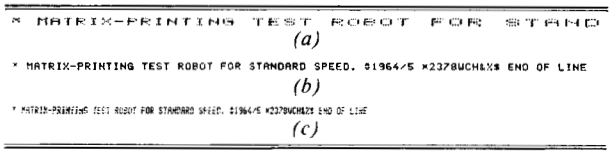

Figure 17 Print samples obtained at 140 char/sec with different paper velocities: (a) 63 cm/sec, (b) 32 cm/sec, and (c) 20 cm/sec. (Size reduced in reproduction.)

demodulation circuit is laid out to give an effective Q of 1000 and a resonant voltage of 40 V. Therefore, an amplitude change of 1 V is obtained for a frequency change of 23 kc/sec (according to F. E. Terman's universal resnance curve).

Returning to our previously calculated values we obtain the following relations: One volt is obtained with a change of 9×10^{-6} pF, using a specimen of 1 mm^2 area at an average distance from the center conductor of the oscillator tank circuit of 1 mm and with a peak-to-peak motion of 2×10^{-6} m. This is ample when dealing with the minute changes of magnetostriction. Figure 18 shows the test setup.

Appendix II

In this appendix the creation of data shown in the "constant-stress resonator design chart" is described. The constant stress shape was developed in individual steps, allowing a modulation depth in stress of 0.1%, being the envelope. Thus, a total of 2300 loops was needed to compute the required data down to a taper of 1%.

Starting with section #1, unit cross-section $Q_n = 1$, the characteristic impedance can be determined as

$$Z_{0_n} = \frac{1}{Q_n} \tag{B1}$$

with the input impedance following the relation

$$X_{I_n} = Z_{0_n} \tan \alpha_I \tag{B2}$$

leading to an input locus

$$\alpha_{I_n} = \text{arc tan} \frac{X_{I_n}}{Z_{0_n}}. \tag{B3}$$

With m as the allowed modulation depth in stress (in our case = 0.999), the actual value of this factor becomes

$$m' = m \cdot \cos \alpha_{I_n}. \tag{B4}$$

The output locus where stress has reduced to 99.9% can be determined as

$$\alpha_{0_n} = \text{arc cos } m', \tag{B5}$$

its impedance being

$$X_{0_n} = Z_{0_n} \tan \alpha_{0_n}. \tag{B6}$$

The length of the first section is then given by

$$\Delta\alpha = \alpha_{0n} - \alpha_{In} \tag{B7}$$

leading to a total length of the tapered portion

$$\alpha_{T_n} = \Sigma\Delta\alpha \tag{B8}$$

with an amplitude of

$$\xi_{T_n} = \alpha_T(0) \cdot \sin 1°. \tag{B9}$$

The pertaining cylindrical piece, needed to complete the tapered part to a quarter wavelength, can now be computed. Its cross section is

$$Q_{n+1} = Q_n \cdot m \tag{B10}$$

and its characteristic impedance

$$Z_{0_{n+1}} = \frac{1}{Q_{n+1}}. \tag{B11}$$

The input impedance of the pertaining piece must be matched to the output impedance of the tapered piece obtained in Eq. (B6):

$$X_{Ip1} = X_{0_n}. \tag{B12}$$

This condition is fulfilled at an input locus

$$\alpha_{Ip1} = \text{arc tan} \frac{X_{Ip1}}{Z_{0_{n+1}}}. \tag{B13}$$

Hence, the length of the pertaining piece is

$$\alpha_{2_{p1}} = 90° - \alpha_{Ip1} \tag{B14}$$

and the amplitude in this portion is

$$\xi_{p1} = 1 - \sin \alpha_{Ip1}. \tag{B15}$$

Figure 18 Measuring device for very small amplitudes.

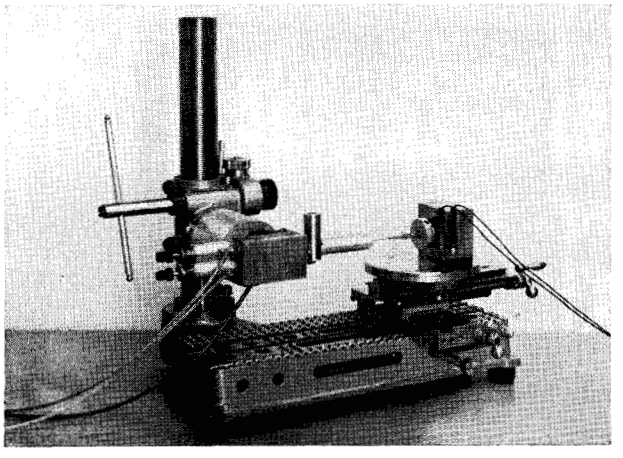

Also, this amplitude is magnified by a factor

$$M = \frac{\xi_{Tn}}{\sin \alpha_{Ip1}} \tag{B16}$$

bringing the total amplitude in the pertaining piece to

$$\xi_{pT1} = M\xi_{p1} \tag{B17}$$

and the total amplitude of the entire resonator to

$$\xi = \xi_{Tn} + \xi_{pT1}. \tag{B18}$$

The relative velocity of sound has increased to

$$V_{SR} = \frac{\alpha_{Tn} + \alpha_{2p1}}{90°} \tag{B19}$$

whereas stress would have decreased to

$$\sigma_n = \frac{1}{\xi_{Tn} + \xi_{pT}} \tag{B20}$$

if the resonator would be used to create unit amplitude.

The available energy is proportional to

$$\epsilon_0 = Q \cdot \xi^2, \tag{B21}$$

whereas the stored energy in the tapered part is

$$\epsilon_{ST} = Q_n \cdot \int_{\alpha = \alpha_{In}}^{\alpha = \alpha_{0n}} \cos^2 \alpha d\alpha \tag{B22}$$

and in the pertaining piece

$$\epsilon_{SP} = Q_{n+1} \cdot \int_{\alpha = \alpha Ip1}^{\alpha = \pi/2} \cos^2 \alpha d\alpha \tag{B23}$$

hence, the total stored energy is

$$\epsilon_S = \epsilon_{SP} + \Sigma\epsilon_{SE}. \tag{B24}$$

The energy ϵ_S remains constant for any degree of taper, therefore the energy throughput is proportional to ϵ_0 with its maximum at a taper of 61%. Returning to step 1 and repeating this procedure 2300 times delivers all data shown in Fig. 8.

References

1. French Patent No. 819843, "Récepteur télégraphique imprimeur à cristal piezoélectrique" by Le Matériel Téléphonique.
2. Warren P. Mason, *Piezoelectric Crystals and Their Application to Ultrasonics*, van Nostrand, 1950.
3. C. M. van der Burgt, "Ferroxcube 7A1 and 7A2, neue piezomagnetische keramische Werkstoffe für Ultraschallschwinger höherer Leistung", *Valvo Berichte*, Band V, Heft 1, (April 1959).
4. E. A. Neppiras, "Very High Energy Ultransonics," *Brit. J. Appl. Phys.* 11, 143 (1960).
5. E. Eisner and J. S. Saeger, "A longitudinally resonant stub for vibrations of large amplitude," *Ultrasonics* **3**, 88 (April–June, 1965).
6. R. Buser, "Vorrichtung zum Sichtbarmachen von in Impulskombinationen vorliegenden Informationen," Deutsche Auslegeschrift No. 1039769.
7. M. Preisinger, "Druckverfahren, bei dem mechanische Schwingungen den eigentlichen Druckvorgang bewirken". German Patent No. 1132158.
8. R. M. Bozorth, *Ferromagnetism*, van Nostrand, 1961.
9. E. Kneller, *Ferromagnetismus*, Springer Verlag, 1962.

Received June 1, 1965